Solid Earth Discuss., 6, 119–144, 2014
www.solid-earth-discuss.net/6/119/2014/
doi:10.5194/sed-6-119-2014

Solid Earth Discussions
Open Access

Observation of a local gravity isosurface by airborne LIDAR of Lake Balaton, Hungary

A. Zlinszky[1,2], G. Timár[3], R. Weber[1], B. Székely[3,4], C. Briese[1,5], C. Ressl[1], and N. Pfeifer[1]

[1]Vienna University of Technology, Department of Geodesy and Geoinformation; Gußhausstraße 27–29, 1040 Wien, Austria
[2]Balaton Limnological Institute, Centre for Ecological Research, Hungarian Academy of Sciences; Klebelsberg Kuno út 3, 8237 Tihany, Hungary
[3]Eötvös Loránd University, Institute of Geography and Earth Science, Department of Geophysics and Space Science; Pázmány Péter Sétány 1/C, 1117 Budapest, Hungary
[4]Interdisziplinäres Ökologisches Zentrum, TU Bergakademie Freiberg, Leipziger Str. 29, 09599 Freiberg, Germany
[5]Ludwig Boltzmann Institute for Archaeological Prospection and Virtual Archaeology; Hohe Warte 38, 1190 Wien, Austria

Received: 3 December 2013 – Accepted: 22 December 2013 – Published: 14 January 2014

Correspondence to: A. Zlinszky (az@ipf.tuwien.ac.at)

Published by Copernicus Publications on behalf of the European Geosciences Union.

Abstract

Airborne LIDAR (Light Detection and Ranging) is a remote sensing method commonly used for mapping surface topography in high resolution. A water surface in hydrostatic equilibrium theoretically represents a gravity isosurface. Here we compare LIDAR-based ellipsoidal water surface height measurements all around the shore of a major lake with a local high resolution geoid model. The ellipsoidal heights of the 87 km^2 we sampled all around the shore of the 597 km^2 lake surface vary by 0.8 m and strong spatial correlation with the geoid undulation was calculated ($R^2 = 0.91$). After subtraction of the local geoid undulation from the measured ellipsoidal water surface heights, their variation was considerably reduced. This demonstrates that the water surface heights of the lake were truly determined by the local gravity potential. We conclude that the accuracy of airborne LIDAR is sufficient for identifying the spatial variations of gravity potential over large inland water surfaces.

1 Introduction

The aim of physical geodesy is the determination of the level surfaces of the Earth's gravity field (Hoffmann-Wellenhof and Moritz, 2005). Lakes are in theory affected by the variations of gravity and the surface of any liquid at rest is part of a surface of equal gravitational potential (Brettenbauer and Weber, 2003; Merriman, 1881; Gomez et al., 2013). Variations in the ellipsoidal height of the standing water surface are therefore expected to correlate closely to variations in geoid undulation. Based on this assumption, mean water levels of lakes have been surveyed with GPS floats (Del Cogliano et al., 2007), water level gauges and satellite altimetry (Cheng et al., 2008) in order to refine local geoid models. River water levels measured by satellite altimetry have been used as a reference for leveling gauge stations (Calmant et al., 2008). Low spatial resolution has always been a difficulty of such studies: radar satellite altimetry involves footprint sizes between 2–10 km (Connor et al., 2009). Satellite laser altimetry offers footprint

SED
6, 119–144, 2014

sizes in range of 50–100 m, but track spacing remains in the range of several tens of kilometers (for temperate latitudes) which still does not allow high-resolution mapping (Baghdadi et al., 2011). The limited range of geoid undulation values encountered within most study areas together with the low spatial resolution of geoid models has also constrained assessment of the correlation between water surface height and geoid undulation, together with the effect of water currents and density differences on surface topography (Hipkin, 2000). A notable exception is the study of Borsa et al. (2008a), who survey a dry salt lake by high resolution GPS topography mapping, and compare the results to local gravity measurements to prove that the salt flat resembles an equipotential surface. While a vehicle-mounted GPS survey over the hard and quasi-stationary surface of a salt flat delivers height accuracies within 2.2 cm (Borsa et al., 2008b), a similar survey on a water surface has to deal with uncertainties in the range of 10–14 cm (Bouin et al., 2009) due to the superposition of waves and dynamic water surface height on patterns of geoid undulation.

We surveyed a lake where the surrounding gravity variations are well understood and have a wide range (> 1 m quasi-geoid height range), using airborne LIDAR for high resolution mapping of the lake surface height. Our objective is to test airborne LIDAR as a novel method for water surface altimetry and to compare the measured pattern of ellipsoidal water surface height with the local quasi-geoid.

Airborne LIDAR is commonly used for mapping terrain topography (Wehr and Lohr, 1999), and stationary laser altimetry has been used for time series measurements of water surface height for radar calibration (Washburn et al., 2011). Airborne LIDAR has also been proven to deliver height measurements comparable with satellite altimetry over sea ice and open water (Connor et al., 2009). Recently, fine-scale height differences caused by internal standing waves in a coastal sea were also mapped by Airborne LIDAR, proving that its accuracy and resolution are suitable for such studies (Magalhaes et al., 2013).

We surveyed Lake Balaton in western Hungary, which is a shallow (average depth 3.3 m), large (597 km^2) and elongated lake of neotectonic origin (Síkhegyi, 2002)

(Fig. 1). The geoid undulation in western Hungary increases along the axis of the Transdanubian Range, a series of hills of NE–SW orientation with elevations 600–700 m a.s.l. Lake Balaton is located on the south-eastern flank of this ridge; therefore the geoid undulation of its immediate neighborhood increases toward the north-west. This trend is explained by the isostatic unbalance of the Transdanubian Range which is a region of ongoing crustal uplift (Fodor et al., 2005; Timár et al., 2005; Síkhegyi, 2002). The center of this process is the axis of the hill chain. Repeated precise leveling has indicated maximum uplift rates of 1 mm/yr^{-1}, with values between 0–0.2 mm/yr^{-1} in the forelands (Joó, 1992). Other methods have suggested slightly lower uplift rates, without disputing the general trend of uplift along the hill chain axis (Szanyi et al., 2009).

2 Method

LIDAR (also known as Airborne Laser Scanning, ALS) is a commonly used remote sensing technique capable of rapidly surveying a large number of points with elevations and horizontal positions accurate to a few cm (Wehr and Lohr, 1999). LIDAR data points are collected with direct georeferencing; i.e. position and attitude of the scanning system are determined by GNSS (Global Navigation Satellite System) once every second and INS (Inertial Navigation System) data are the basis for interpolation within this time interval, separately and independently for each laser pulse. GNSS allows to determine the scanner position in geocentric Cartesian coordinates within the reference frame of the base station. These Cartesian coordinates are first converted to ellipsoidal latitude, longitude, and height (Hoffmann-Wellenhof and Moritz, 2005) and then projected to plane grid coordinates and ellipsoidal height. This process does not involve a geoid model, nor is it affected by gravity variations.

We measured elevation of the lake water surface by 59 flight strips along the whole shoreline (Fig. 2a and b). Since the main goal of the survey was littoral vegetation mapping (Zlinszky et al., 2012), the flight pattern was optimized for continuous coverage of the coast and the coastal water surface. A Leica ALS 50 laser scanner operating at

1064 nm (Zlinszky et al., 2011, 2012) was used with a stripwise nominal ground point density of 1 point m^{-2} at the average flying height of 1400 m above ground. The strip width varied between 600 and 1200 m and neighboring strips had an average overlap of 15 %. The data were delivered in the global geodetic datum in UTM projection and this coordinate system was used throughout the study.

We used LIDAR strip adjustment (Filin, 2003; Kager, 2004; Ressl et al., 2011; Skaloud and Lichti, 2007) to improve the relative georeferencing of the flight strips by optimizing their relative alignment with respect to each other. In the first step, inclined planar surfaces (typically building roofs) were extracted automatically from the LIDAR points in each strip. During an iterative process, misalignment, lever arm, offset, scale, deflection angle, and individual global shifts of each strip were estimated in order to minimize the differences between corresponding planes in the overlapping parts of each pair of strips. The adjustment delivered optimal values for these parameters which we then used to transform all the LIDAR points of each strip to new locations. The shifts were determined independently from eventual water level variations as they were calculated only from selected shore features. Typical shifts were less than 20 cm.

The OPALS software package (Pfeifer et al., accepted, 2013; Mandlburger et al., 2009) was used for interpolation and processing. Moving least squares interpolation with a plain model was applied for creating a raster elevation model of the water surface with 1 m × 1 m raster resolution. We used the lake outline and a vegetation map generated from the ALS data (Zlinszky et al., 2012) to remove the non-water areas. Visual quality control showed that cells with ellipsoidal heights lower than 149.5 m or higher than 152 m are mostly artifacts, mainly high points from vegetation, boats etc. Therefore, cells with ellipsoidal elevations outside these limits were also excluded from further study (1 % of the LIDAR raster cells). As the height distribution contained some outliers (remaining non-water points), standard deviation would not have yielded a representative value. Therefore σ_{MAD} was used as robust estimator of the standard deviation. It is defined as $\sigma_{\mathrm{MAD}} = 1.426 \cdot \mathrm{MAD}$, where MAD is the median of the absolute deviation to the median. For a normal distribution σ_{MAD} is equal to the standard deviation.

In order to correct for short-term local water level variations of the lake during the survey, measurements of the water gauge network around the lake were investigated. These were collected at 9 stations in 15 min intervals, using floats connected to digital recorders (3 stations) or pressure sensors (6 stations). In order to remain independent from the datum surface of the water gauges (which is a geoid model in itself), the local mean lake level (LMLL) during the 4 days of flight was calculated separately for each gauge. A time series of water level variations compared to the LMLL was calculated for each measuring station. This series was compared with GPS time recordings of each flight strip, and the ellipsoidal height of the elevation model pixels within each flight strip corrected with the difference between LMLL and local water level, measured exactly at the place and time of the strip. Correction values were between −6 and +2.5 cm, with a median of +0.16 cm and a σ_{MAD} of 1.31 cm. As a result, a water surface model was produced, with approximately 87 million data points characterized by horizontal coordinates and adjusted elevations above the WGS 84 ellipsoid.

As a basis for comparison with the local gravity isosurface the HGEO2000 Hungarian quasi-geoid model (Kenyeres, 1999; Kenyeres, 2000; Völgyesi et al., 2005) and the HGTUB2007 Hungarian quasi-geoid model (Tóth, 2009a, b) were considered, and HGTUB2007 was chosen due to its finer spatial resolution. We are aware that the quasi-geoid is not necessarily an equipotential surface, however, the Hungarian National Height system uses normal heights, and normal heights within Hungary deviate max. 2.8 cm from orthometric heights (Ádám, 1999), which is within LIDAR measurement accuracy. The calculation of HGTUB2007 is described in full detail in Tóth (2009b). Tóth (2009b) calculated the quasi-geoid from the following data sets: 6678 mean free-air gravity anomalies in $2' \times 3'$ blocks based on more than 300 000 point gravity data; 276 vertical deflection components based on 138 astrogeodetic vertical deflections (both North and East component); 7452 surface gravity gradients (torsion balance stations) resampled from 27 005 measurement points; and 94 GPS leveling measurements of the Hungarian National GPS network (OGPSH). The GPM98CR geopotential model was combined with the GRACE GGM02C model to the maximum degree and order 720 and used for reduction of the observations. RTM corrections were calculated based on the fixed mass model of SRTM3 heights. The residual gravity field of all observations was interpolated by least squares collocation with the self-consistent logarithmic covariance model of Forsberg (1987), to a grid of $1.5' \times 1'$ resolution. The estimated prediction errors of the model are below 2 cm inside Hungary (Tóth, 2009).

For comparison with the quasi-geoid model, the LIDAR-derived (and water level corrected) water surface model had to be resampled to the same spatial resolution. In order to ensure that the remaining elevated non-water points in the data do not distort the heights, the 30th percentile of the water surface model cell heights within each cell of the quasi-geoid model was calculated and used for representing the water surface heights. As a further correction, cells that did not represent the water surface height because they were mainly over shore or wetland surfaces were removed excluding 16 of the originally 207 data points, removing the imperfections of land and vegetation masking. The correlation of this low-resolution water surface height model with the quasi-geoid was tested by linear regression.

3 Results

The 87 077 358 raster cells had an elevation range of 80 cm. The largest ellipsoidal elevations of the water surface model are in the north-western basin of the lake, decreasing gradually toward the southern shore with the lowest areas in the south-western corner. The ellipsoidal heights of the water surface in overlapping areas of strips surveyed on different days were similar within the accuracy of the instrument ($\sim$ 5 cm). Water levels measured during the flight window showed some variation (explained in detail in Appendix A), with a total range of 20 cm for all stations. Water level deviations from LMLL measured synchronously with the flight strips have a total range of ±6.0 cm for the four flight days (Fig. 4).

SED
6, 119–144, 2014

We created a simple gravity isosurface model by adding a constant (105.1 m, mean height of the lake surface above sea level) to the quasi-geoid height raster, considering the difference between orthometric and normal heights negligible for our study. Comparing this gravity isosurface model throughout the area of the lake with the measured ellipsoidal water surface elevations shows close correlations (Fig. 2a, see also Supplement). The geoid undulation difference between the shores of the lake corresponds to the water surface elevation pattern in flight strips both parallel and perpendicular to the shore. The ellipsoidal height range of the water surface heights was approximately 80 cm, with a dispersion (quantified by σ_{MAD}) of 20 cm (Fig. 2a). The water surface heights resampled to the geoid model resolution were compared with the geoid undulation of each cell: a linear regression with an R^2 value of 0.906 was calculated with a slope of 1.12, intercept of 99.95 m and σ_{MAD} of 5.17 cm. This agrees with our expectation that the pattern of water surface ellipsoidal heights is explained by the height variations of the gravity isosurface.

When the local quasi-geoid heights were resampled by bilinear interpolation to the spatial resolution of the water surface model (1 m × 1 m) and subtracted from the local water surface model elevations, the σ_{MAD} was reduced to 5.6 cm, and the elevation range of the water points to 30 cm. 78 % of the points were within 15 cm and 36.1 % of the 87 000 000 points within 5 cm (Fig. 2b, see also Supplement). Hardly any flights strips show along-track differences, not even those spanning 15 cm of quasi-geoid height range along their length. The geoid-corrected water surface heights are slightly lower than average in the SE corner of the lake and higher than average in the NW, a pattern that suggests that the height gradient of the lake may be even steeper than the gradient in the quasi-geoid model.

This is confirmed by the scatterplot of the measured ellipsoidal water surface heights and the corresponding geoid undulation (Fig. 3). A clear linear trend is visible, and the slope is very close to 1 (1.06), which agrees with our expectation that the geoid undulation controls water surface height variation in space. Nevertheless, water surface heights show a steeper profile than the geoid model, and fall steeply below the 1 : 1

SED
6, 119–144, 2014

line for the lower quasi-geoid height values. Erroneously high or low artifact points are probably created by non-water features insufficiently removed.

4 Error Budget

For the LIDAR data of Lake Balaton no geometric ground control features were available, therefore the absolute georeferencing accuracy is a product of standard differential GNSS georeferencing (10 cm according to the flight operator). However, the relative georeferencing of the strips (i.e. their mutual alignment) was improved by strip adjustment, as documented by σ_{MAD} and the 70th percentile of the differences in smooth areas of overlapping strip pairs. For all considered 305 pairwise strip differences (with around 106 000 000 difference values in total) σ_{MAD} improved from 12 cm (before) to 5 cm (after strip adjustment). The 70th percentile of the absolute differences improved from 16 cm (before) to 4 cm (after).

Single water gauge measurements can be considered accurate within a centimeter, but the LMLL as a datum surface is less accurate. Calculated as an average of the local water levels measured every 15 min during the four days of flight, the errors of LMLL can be estimated from the range of local mean water levels calculated separately for each measurement day and each gauge. This is below 2 cm for all stations, and below 1 cm for 6 out of 9 stations.

A possible source of error in the height measurements was water as the target surface for LIDAR. Over calm (flat) water surfaces, specular reflection dominates, which means that for most of the strip, the pulse energy is reflected away from the sensor, with an insufficient return for triggering the detector and therefore no recorded point. At nadir and again over calm water, the pulse energy reflected specularly arrives back in the sensor, producing a point and also often a glint effect. This is known to result in slightly shorter range measurements (10–50 cm), as the high amount of incoming energy results in the system detecting a peak too early (range-walk effect). For most of the flight campaign the moderate waves encountered were sufficient to produce non-specular reflection and therefore correct measured ranges, while glint range-walk effects were encountered in less than 1 % of the data. Regardless of the target surface, the range measurement accuracy also varies with scan angle: at the edge of the strip, the elevations measured are slightly less accurate. The typical result of this, as observed, is that measurement points from strip edges can be up to 5 cm lower than the strip centerline.

While over oceans, dynamic water surface topography is known to include deviations from the gravity-driven equilibrium of more than a meter (Seeber, 2003), this is much less prominent in a lake because of the shallow depth (3.3 m on average) and low current intensity at the time of flight.

Storms can produce disequilibrium of the lake surface, increasing the water level on the downwind side while decreasing it upwind (setup) or producing dynamic standing waves along or across the lake, with wavelengths of several kilometers (seiche). In case of Lake Balaton, this starts at sustained wind speeds above 5 $m\,s^{-1}$ and such a displacement can reach 1 m in water level during storms winds of 20 $m\,s^{-1}$ (Muszkalay, 1973; Somlyódy, 1983). According to local Meteorological Aerodrome Report (METAR) data, wind speeds never exceeded 5 $m\,s^{-1}$ during the whole survey. Some setup and seiche effects can be observed in the water level data (see Appendix A and Fig. 4), but these were corrected for as described in the methodology. The slope driving the flow of water along the lake from the tributary rivers to the outlet could be suspected as the reason for the ellipsoidal height differences. However, the turnaround time for water in the lake is more than two years (Somlyódy, 1983), so the flow is very weak. The patterns observed in ellipsoidal height do not match the main tributaries or the outlet of the lake. This means seiche or mass flow can be ruled out as a cause for the measured ellipsoidal height differences of the water surfaces, and after applying the corrections for deviations from LMLL, our height model of the water surface of the lake can be regarded to represent on the scale of the whole lake, the state of hydrostatic equilibrium.

The remaining elevation variations may result from the inaccuracy of the geoid model which involves spatial smoothing (around 2 cm), the difference between the quasi-geoid based equipotential surface model and the true isosurface (around 2 cm) the residual error of the relative georeferencing (5 cm), local waves (which do not influence the mean height), or sensor artifacts where such a large-scale pattern can be excluded.

5 Discussion and conclusions

Comparison of water surface ellipsoidal heights with the quasi-geoid model shows that these correlate very closely, with 90.1 % of the variations in water surface height explained by the quasi-geoid height variations. As far as the resolution of the geoid model allowed, the close correlation of the two data systems confirmed that standing water has a truly level surface. Variations in the ellipsoidal height of the lake water surface are mainly a product of the variations in local gravity potential represented by the geoid undulation; the slight water level changes induced by movement of water during the flight period were corrected for. One of the limitations of the correlation is the resolution of the geoid model we used: similar to satellite altimetry, the resolution of the water surface is much higher than the resolution of the geoid model, therefore limiting comparison (Cheng et al., 2008). However, the high resolution of the LIDAR-derived water surface model shows even shorter wavelength patterns in height, and therefore potentially in geoid undulation, which are beyond the scale of the geoid model. This implies that water surface ellipsoidal heights measured by LIDAR might be used in the future to refine local gravity variation models. The theory of hydrostatic equilibrium being connected over large areas to the local gravity field has already been exploited for surveying the geoid over the oceans (such as ICESat and Envisat), but these measurements are affected by dynamic ocean topography (Hoffmann-Wellenhof and Moritz, 2005). In our case, the dense network of water level gauges and the high measurement frequency allowed quantification of dynamic water height effects and correction of any measurement bias. This was possible since only water surfaces close to the shore were surveyed and because the flight took place under calm weather conditions. Our LIDAR measurement accuracy of 5 cm calculated from flat terrestrial surfaces after strip adjustment compares to the 4 cm accuracy obtained by Borsa et al. (2008b) through vehicle-mounted GPS surveys (over much larger area), and to the best accuracies measured from ship-mounted GPS under calm weather conditions (10 cm) (Bouin et al., 2009), but are slightly worse than the 2.7 cm error reached with a GPS catamaran in a marine setting by Bonnefond et al. (2003). Borsa et al. (2008a) find that 93 % of the ellipsoidal height variations of a dry salt flat are explained by variations in geoid height, and come to the conclusion that the surface topography closely approximates the gravity equipotential surface. At the scale of the most detailed quasi-geoid model we could obtain, we found that 90.1 % of the water surface topography variation is explained by variations in quasi-geoid height.

Point elevation measurements from GNSS buoys were already used as part of a leveling-based geoid survey (Gomez et al., 2013), and satellite gravimetry-based geoid change measurements have been used as a proxy for lake water levels (Awange et al., 2008; Calmant et al., 2008). However, active satellite altimeters were only applied in rare cases for mapping inland lakes as level surfaces, probably mainly because of their limited spatial resolution (Hoffmann-Wellenhof and Moritz, 2005; Cheng et al., 2008; Baghdadi et al., 2011).

Comparing satellite altimetry with terrestrial, airborne and satellite gravimetry over the Great Lakes Kingdon et al. (2008) observe that lake surface altimetry follows short wavelength gravity anomalies confirmed by ship- or airborne gravimetry better than GRACE satellite measurements. They also describe the absolute accuracy of the altimetry-derived quasi-geoid to be closer to the GRACE values than the high resolution ship- or airborne measurements, which were more prone to systematic bias. This means that altimetry is more accurate than terrestrial gravimetry but delivers higher resolutions than satellite gravimetry. If the same principles apply to LIDAR, which is also based on altimetry, it can be expected that LIDAR-derived lake surface heights would deliver a valuable input to high-resolution geoid models. Compared to satellite altimetry, LIDAR is characterized by smaller footprints, even higher spatial resolutions and the possibility to survey large areas within a few hours. Similarly to satellite altimetry over oceans, the spatial resolution and area coverage of LIDAR could theoretically allow identification of dynamic water topography features of lakes such as plumes or eddies. Since our data only covered the waters nearest to the shore, and since the lake was near equilibrium, this could not be tested in our case.

Compared to GPS buoys which collect height data spread over longer periods to assess mean lake level, LIDAR delivers repeated measurements spread in space. This has comparable accuracy to the technique of Bonnefond et al. (2003) who used GPS receivers mounted on ships to obtain area-covering sea level height measurements, but is more productive due to higher survey speeds and area coverage. However, LIDAR surveys provide a snapshot and are thus more easily distorted by the effects of water movement, requiring correction based on local water stages. The method we proposed only needs relative height changes at each gauge.

Compared to analysis of simultaneous water level gauge readings such as Cheng et al. (2008), the advantage of LIDAR in our case is the higher number of data points, which deliver statistically stronger results while using coverage of the shore for accurate relative georeferencing. It is expected that in the future, LIDAR coverage of lake surfaces will further increase with the spread of bathymetric LIDAR (Mandlburger et al., 2011).

The typical methods for assessing geoid undulations over land are gravimetry and the surveying of leveled elevation benchmarks with GNSS (Seeber, 2003). A drawback of these techniques is the limited number of possible measurement points confining spatial resolution and noise removal. In our case the lake itself serves as a leveling instrument providing a vast area where elevations relative to the geoid are shown to be constant. In combination with the high resolution of LIDAR and the improved accuracy of strip adjustment, an adequate signal to noise ratio is reached.

We conclude that LIDAR mapping of lake surface elevations can deliver information on the ellipsoidal height pattern of the water surface, and thus on the local gravity

SED
6, 119–144, 2014

anomalies. These in turn can be used to collect information about the formation of the lake (Dietrich et al., 2013). LIDAR surveying of lakes can be valuable for estimating the error budget of lower resolution regional geoid models and GPS-derived heights calculated based on such models. Since many major European and North American lake shores have already been surveyed by LIDAR, there is a wealth of data available.

Appendix A: Water levels of Lake Balaton during the studied period

Investigation of the water levels of the lake will be used to answer two questions:

(i) To what extent was the lake at hydrostatic equilibrium during the airborne survey?

(ii) How did variations in local lake water levels affect the ellipsoidal heights measured by LIDAR?

Hydrostatic equilibrium would mean that the lake was free from dynamic processes such as local currents, eddies and standing waves, and therefore the rules of hydrostasis would govern the pattern of its surface elevation. Whether the lake was in such a state can be decided based on local water level variations. The common datum of water gauges around the lake was defined based on a geoid model, therefore it is subject to errors of the model and might not perfectly represent the true long-term surface of the lake in theoretical equilibrium. Therefore, we studied water level changes independently for each gauging station: local mean lake levels for each station are expected to define this equilibrium across long-term measurements. During the four days of our flight, the daily LMLL-s showed increases or decreases of a few centimetres, therefore it was assumed that slight changes of lake water volume are affecting these measurements (Fig. 4). In this case, measuring LMLL across longer periods of time might not necessarily have increased the accuracy of LMLL estimation.

While wind and currents of lakes are known to induce static and also periodic deviations from the equilibrium water level (“setup” and “seiche”), the wind speeds observed

SED
6, 119–144, 2014

during the campaign are below the known threshold for such processes (Muszkalay, 1973). The flight data was collected during the days 21, 22, 23 and 26 August 2010. 24 and 25 were left out because of cloudy weather. During day 1, the highest water level, 122 cm above the station datum (8 cm above LMLL) was observed in Keszthely, where the water level slowly fluctuated between 112 and 122 cm with a period of ca. 5 h. While this periodic fluctuation with decreasing amplitude implies a standing wave (seiche), no water gauge showed the same movement in opposite direction. It is already known that the Keszthely gauge typically records the largest dynamic water level variations, since the small western basin of the lake is the most sensitive to the wind. This fluctuation was most probably caused by remnants of seiche from winds during the previous day (Fig. 4).

The lowest water level for day 1, 103 cm (9 cm below LMLL) was observed in Tihanyrév in the Tihany straits and is an isolated low record both preceded and followed by continuous recordings around 111 cm (0.7 cm below LMLL). This pattern matches some measurements described by Muszkalay (1973) as a short-term standing wave forming within a harbour basin, which might well be the case since Tihanyrév has intensive ferryboat traffic. Neither of these deviations corresponded to the flight times of Day 1; in fact, during the afternoon flight the water level was within 2 cm to LMLL for all stations near the flight area of the day (Fig. 4).

During day 2, the highest recorded water level deviation was 5 cm above the LMLL, again an isolated measurement of 117 cm in Tihanyrév preceded and followed by values around 112 cm. The lowest level is −1.9 cm below LMLL, 110 cm measured at Siófok, preceded and followed by readings of 111 cm. During the time of the flight on that day, the deviation from LMLL was between −1.8 and +2.3 cm for the stations covered by the flight area (Fig. 4).

During day 3, the highest differences to LMLL of +3.3 cm were measured over the course of an hour in the evening in Balatonfűzfő; not counting an isolated reading of +4.2 cm in the Tihanyrév harbour. The largest negative difference to LMLL was −2.9 cm in Siófok, sustained during several hours at night. The minimum −2.7 cm compared to

SED
6, 119–144, 2014

LMLL (111 cm above gauge datum) was continuously measured during the morning hours of the day in Keszthely. During the flight, deviations from LMLL were between −1.8 and +3.3 cm (Fig. 4).

During day 4, the largest absolute differences with respect to LMLL were +10.3 and −7.7 cm, both observed in Keszthely. Here the water level rose from 114 cm (above the gauge datum) during 2 h to 124 cm and fell back to 112 in the next two hours. The largest negative deviation (−7.7 cm) happened during the flight in Keszthely, the largest positive difference to LMLL was +2.1 cm in Siófok (Fig. 4).

Apparently, even under calm conditions, standing waves and other dynamic processes can cause up to 10 cm differences compared to the average water level. The strongest fluctuations were observed in Keszthely and Balatonfűzfő, which are both near the ends of the lake and in narrow corners capable of producing water level changes higher than on the open lake surface due to a funnel effect. If this is the case and the lake level changes amplified by the funnel effect reach no more than 10 cm differences compared to the average water level, we can only expect minor dynamic lake topography along the more open shores. We thus conclude that while the lake was not at full hydrostatic equilibrium during the flight days, dynamic local water level changes were within ±5 cm for most measurement sites, and within ±10 cm globally. Due to high frequency water level measurements and some luck in the timing of most flights to the afternoons, the dynamic water level variations actually affecting our measurements were typically even lower, typically within ±3 cm, in one isolated case reaching −7.7 cm. These variations were relatively well understood and corrected for by measuring deviations from LMLL at 9 stations with 15 min frequency.

The Supplement related to this article is available online at doi:10.5194/sed-6-119-2014-supplement.

Acknowledgements. The airborne survey of the Lake was sponsored by the European Community's 7th Framework programme (FP7/2008-20012) under EUFAR contract No. 2271; strip adjustment was funded by the GIONET FP7 project (PITN-GA-2010-264509). AZ and partly BSz and NP were funded by the Changehabitats2 FP7 project, CB by the Ludwig Boltzmann Institute, BSz contributed as an Alexander von Humboldt Research Fellow. Contribution of GT was partially supported by the Hungarian National Research Fund (OTKA) project NK83400, AZ was partially supported by the project TÁMOP-4.2.2.A-11/1/KONV-2012-0064, "Regional effects of weather extremes resulting from climate change and potential mitigation measures in the coming decades". The HGTUB2007 geoid model was kindly provided by Gyula Tóth from the Department of Geodesy and Surveying of the Budapest University of Technology and Economics.

References

Ádám, J.: Difference between geoid undulation and quasigeoid height in Hungary, Bolletino di Geofisica Teorica e Applicata, 40, 571–575, 1999.

Awange, J. L., Sharifi, M. A., Ogonda, G., Wickert, J., Grafarend, E. W., and Omulo, M. A.: The falling Lake Victoria water level: GRACE, TRIMM and CHAMP satellite analysis of the lake basin, Water Resour. Manag., 22, 775–796, doi:10.1007/s11269-007-9191-y, 2008.

Baghdadi, N., Lemarquand, N., Abdallah, H., and Bailly, J. S.: The relevance of GLAS/ICESat elevation data for the monitoring of river networks, Remote Sens., 3, 708–720, doi:10.3390/rs3040708, 2011.

Bonnefond, P., Exertier, P., Laurain, O., Menard, Y., Orsoni, A., Jeansou, E., Haines, B. J., Kubitschek, D. G., and Born, G.: Leveling the sea surface using a GPS-catamaran, Mar. Geod., 26, 319–334, doi:10.1080/01490410390256673, 2003.

Borsa, A. A., Bills, B. G., and Minster, J.-B.: Modeling the topography of the salar de Uyuni, Bolivia, as an equipotential surface of Earth's gravity field, J. Geophys. Res.-Sol. Ea., 113, 1–21, doi:10.1029/2007jb005445, 2008a.

Borsa, A. A., Fricker, H. A., Bills, B. G., Minster, J.-B., Carabajal, C. C., and Quinn, K. J.: Topography of the salar de Uyuni, Bolivia from kinematic GPS, Geophys. J. Int., 172, 31–40, doi:10.1111/j.1365-246X.2007.03604.x, 2008b.

Bouin, M.-N., Ballu, V., Calmant, S., Bore, J.-M., Folcher, E., and Ammann, J.: A kinematic GPS methodology for sea surface mapping, Vanuatu, J. Geodesy, 83, 1203–1217, doi:10.1007/s00190-009-0338-x, 2009.
Brettenbauer, K. and Weber, R.: A primer of geodesy for GIS users, Geowissenschaftliche Mitteilungen, 64, 1–55, 2003.
Calmant, S., Seyler, F., and Cretaux, J. F.: Monitoring continental surface waters by satellite altimetry, Surv. Geophys., 29, 247–269, doi:10.1007/s10712-008-9051-1, 2008.
Cheng, K.-C., Kuo, C.-Y., Shum, C. K., Niu, X., Li, R., and Bedford, K. W.: Accurate linking of Lake Erie water level with shoreline datum using GPS buoy and satellite altimetry, Terr. Atmos. Ocean. Sci., 19, 53–62, doi:10.3319/tao.2008.19.1-2.53(sa), 2008.
Connor, L. N., Laxon, S. W., Ridout, A. L., Krabill, W. B., and McAdoo, D. C.: Comparison of Envisat radar and airborne laser altimeter measurements over Arctic sea ice, Remote Sens. Environ., 113, 563–570, doi:10.1016/j.rse.2008.10.015, 2009.
Del Cogliano, D., Dietrich, R., Richter, A., Perdomo, R., Hormaechea, J. L., Liebsch, G., and Fritsche, M.: Regional geoid determination in Tierra del Fuego including GPS levelling, Geol. Acta, 5, 315–322, 2007.
Dietrich, V. J., Lagios, E., Reusser, E., Sakkas, V., Gartzos, E., and Kyriakopoulos, K.: The enigmatic Zerelia twin-lakes (Thessaly, Central Greece): two potential meteorite impact Craters, Solid Earth Discuss., 5, 1511–1573, doi:10.5194/sed-5-1511-2013, 2013.
Filin, S.: Recovery of systematic biases in laser altimetry data using natural surfaces, Photogramm. Eng. Rem. S., 69, 1235–1242, 2003.
Fodor, L., Bada, G., Csillag, G., Horváth, E., Ruszkiczay-Rüdiger, Z., Palotás, K., Síhegyi, F., Timár, G., Cloetingh, S., and Horvath, F.: An outline of neotectonic structures and morphotectonics of the western and central Pannonian Basin, Tectonophysics, 410, 15–41, 2005.
Forsberg, R.: A new covariance model for inertial gravimetry and gradiometry, J. Geophys. Res.-Solid, 92, 1305–1310, doi:10.1029/JB092iB02p01305, 1987.
Gomez, M. E., Del Cogliano, D., and Perdomo, R.: Geoid modelling in the area of Fagnano Lake, Tierra del Fuego (Argentina): insights from mean lake-level observations and reduced gravity data, Acta Geod. Geophys. Hu., 48, 139–147, doi:10.1007/s40328-012-0009-x, 2013.
Hipkin, R.: Modelling the geoid and sea-surface topography in coastal areas, Phys. Chem. Earth Pt. A, 25, 9–16, doi:10.1016/s1464-1895(00)00003-x, 2000.
Hoffmann-Wellenhof, B. and Moritz, H.: Physical Geodesy, Springer Wien NewYork, Wien, Austria, 397 pp., 2005.

SED
6, 119–144, 2014

Joó, I.: Recent vertical surface movements in the Carpathian Basin, Tectonophysics, 202, 129–134, 1992.
Kager, H.: Discrepancies between overlapping laser scanning strips – Simultaneous fitting of Aerial Laser Scanning strips, International Society for Photogrammetry and Remote Sensing XXth Congress, Istanbul, 12 July 2004, 2004.
Kenyeres, A.: Completion of the nationwide GPS-gravimetric geoid solution for Hungary, Phys. Chem. Earth Pt. A, 24, 85–90, doi:10.1016/s1464-1895(98)00015-5, 1999.
Kingdon, R., Hwang, C., Hsiao, Y.-S., and Santos, M.: Gravity anomalies from retracked ERS and Geosat altimetry over the Great Lakes: accuracy assessment and problems, Terr. Atmos. Ocean. Sci., 19, 93–101, doi:10.3319/tao.2008.19.1-2.93(sa), 2008.
Magalhaes, J. M., da Silva, J. C. B., Batista, M., Gostiaux, L., Gerkema, T., New, A. L., and Jeans, D. R. G.: On the detectability of internal waves by an imaging lidar, Geophys. Res. Lett., 40, 3429–3434, doi:10.1002/grl.50669, 2013.
Mandlburger, G., Hauer, C., Höfle, B., Habersack, H., and Pfeifer, N.: Optimisation of LiDAR derived terrain models for river flow modelling, Hydrol. Earth Syst. Sci., 13, 1453–1466, doi:10.5194/hess-13-1453-2009, 2009.
Mandlburger, G., Pfennigbauer, M., Steinbacher, F., and Pfeifer, N.: Airborne Hydrographic LiDAR Mapping – Potential of a new technique for capturing shallow water bodies, 19th International Congress on Modelling and Simulation, edited by: Chan, F., Marinova, D., and Anderssen, R. S., 2416–2422, 2011.
Merriman, M.: Figure of the Earth – an Introduction to Geodesy, John Wiley and Sons, New York, 88 pp., 1881.
Muszkalay, L.: A Balaton vizének jellemző mozgásai, Vízgazdálkodási Tudományos Kutató Intézet, Budapest, 85 pp., 1973.
Pfeifer, N., Mandlburger, G., Otepka, J., and Karel, W.: OPALS – a framework for airborne laser scanning data analysis, Comput. Environ. Urban, in press, doi:10.1016/j.compenvurbsys.2013.11.002, 2013.
Ressl, C., Pfeifer, N., and Mandlburger, G.: Applying 3D affine transformation and least squares matching for airborne laser scanning strips adjustment without GNSS/IMU trajectory Data, ISPRS Workshop Laser Scanning 2011, Calgary, Canada, 2011.
Seeber, G.: Satellite Geodesy, 2 Edn., de Gruyter, Berlin, 589 pp., 2003.

SED
6, 119–144, 2014
Airborne LIDAR of lake as gravity isosurface
A. Zlinszky et al.

Síkhegyi, F.: Active structural evolution of the western and central parts of the Pannonian basin: a geomorphological approach, EGU Stephan Mueller Special Publication Series, 3, 203–216, 2002.

Skaloud, J. and Lichti, D.: Rigorous approach to bore-sight self-calibration in airborne laser scanning (vol 61, pg 47, 2006), ISPRS J. Photogramm., 61, 414–415, doi:10.1016/j.isprsjprs.2006.11.001, 2007.

Somlyódy, L.: Major features of the Lake Balaton eutrophication problem: approach to the analysis, in: Eutrophication of Shallow Lakes: Modeling and Management – The Lake Balaton Case Study, edited by: Somlyódy, L., Herodek, S., and Fischer, J., IIASA collaborative proceedings series, International Institute for Applied Systems Analysis, Laxenburg, Austria, 1983.

Szanyi, G., Bada, G., Surányi, G., Leél-Össy, S., and Varga, Z.: A Budai-hegység pleisztocén kiemelkedéstörténete barlangi lemezes kalcitkiválások urán-soros kormeghatározása alapján, Földtani Közlöny, 139, 353–366, 2009.

Timár, G., Kis, K., and Kenyeres, A.: Short-wavelength component of the geoid: a possible indicator of the isostatic character, Geophys. Res. Abst., 7, 02636, SRef-ID:1607-7962/gra/EGU05-A-02636, 2005.

Tóth, G.: New Combined Geoid Solution HGTUB2007 for Hungary, in: Observing Our Changing Earth, edited by: Sideris, M. G., International Association of Geodesy Symposia, IAG Symposia vol 133, Springer, Berlin, Heidelberg, 405–412, 2009a.

Tóth, G.: A HGTUB2007 új magyarországi kombinált kvázigeoid megoldás, Geomatikai Közlemények, 12, 131–140, 2009b.

Völgyesi, L., Kenyeres, A., Papp, G., and Tóth, G.: A geoidmeghatározás jelenlegi helyzete Magyarországon, Geodézia és Kartográfia, 57, 4–11, 2005.

Washburn, S. A., Haines, B. J., Born, G. H., and Fowler, C.: The harvest experiment LIDAR system: water level measurement device comparison for Jason-1 and Jason-2/OSTM calibration, Mar. Geod., 34, 277–290, doi:10.1080/01490419.2011.590114, 2011.

Wehr, A. and Lohr, U.: Airborne laser scanning – an introduction and overview, ISPRS J. Photogramm., 54, 68–82, 1999.

Zlinszky, A., Tóth, V., Pomogyi, P., and Timár, G.: Initial report of the AIMWETLAB project: simultaneous airborne hyperspectral, LIDAR and photogrammetric survey of the full shoreline of Lake Balaton, Hungary, Geographia Technica, 11, 101–117, 2011.

Zlinszky, A., Mücke, W., Lehner, H., Briese, C., and Pfeifer, N.: Categorizing wetland vegetation by Airborne Laser Scanning on Lake Balaton and Kis-Balaton, Hungary, Remote Sens., 4, 1617–1650, doi:10.3390/rs4061617, 2012.

SED
6, 119–144, 2014

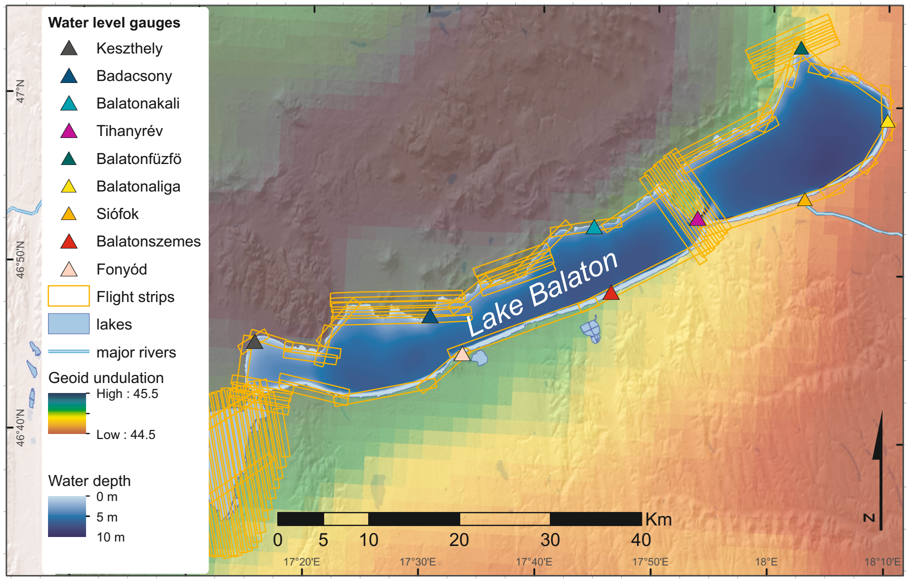

Figure 1. Map of the study area, including quasi-geoid heights, bathymetry of Lake Balaton and flight pattern. Terrain topography is represented by relief shading. Note quasi-geoid high NW of the lake.

SED
6, 119–144, 2014

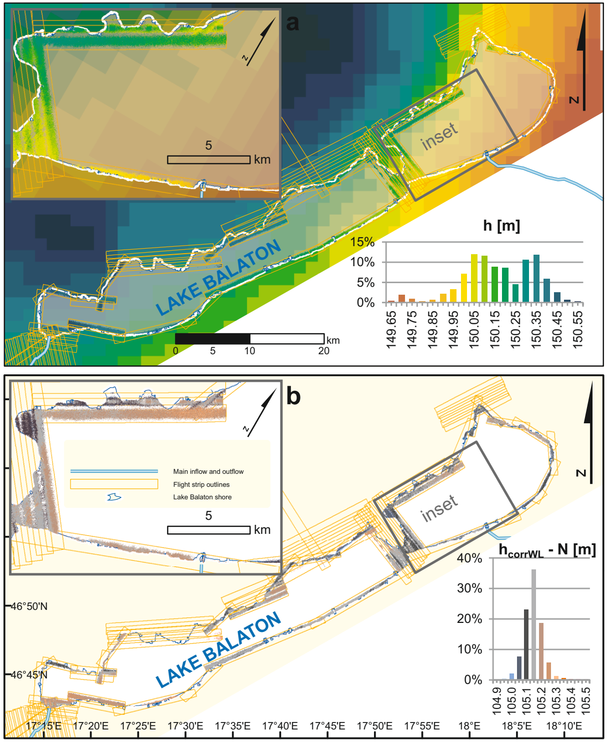

Figure 2. Scatterplot of water surface ellipsoidal heights (corrected with deviation of local water level from LMLL) with respect to local quasi-geoid height. Scatterplot cell colouring shows point count for each ellipsoidal water height/quasi-geoid height interval of 1.25 × 1.25 cm. Bilinear interpolation of geoid undulation raster to LIDAR resolution was used for this graph. Crosses show water surface and quasi-geoid height data points resampled to quasi-geoid model resolution as used for calculating regression.

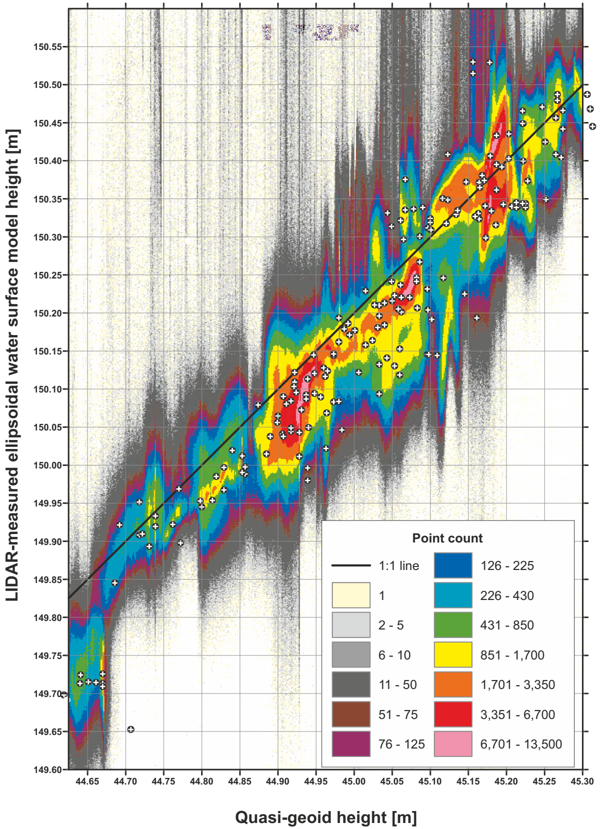

Figure 3. Scatterplot of water surface ellipsoidal heights (corrected with deviation of local water level from LMLL) with respect to local quasi-geoid height. Scatterplot cell colouring shows point count for each ellipsoidal water height/quasi-geoid height interval of 1.25 × 1.25 cm. Bilinear interpolation of geoid undulation raster to LIDAR resolution was used for this graph. Crosses show water surface and quasi-geoid height data points resampled to quasi-geoid model resolution as used for calculating regression.

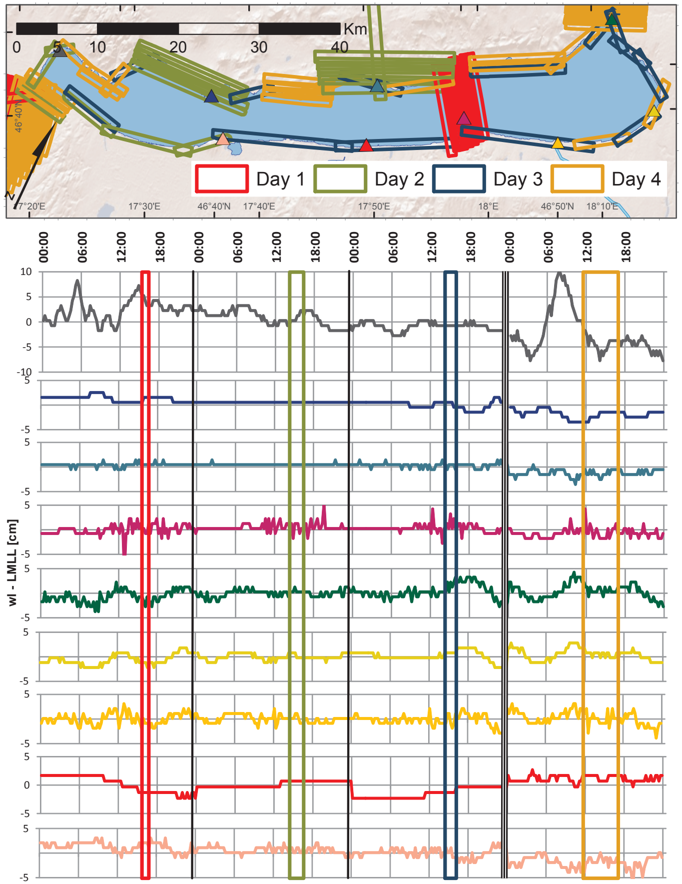

Figure 4. Water level recordings with respect to local mean lake level of all 9 water level gauges around Lake Balaton, during the 4 days of flight. Triangles in the map depict the water gauges (colour coded to the water level graphs), rectangles crossing all graphs show actual flight times of LIDAR strips.

SED
6, 119–144, 2014